BJR

Received:
19 November 2015

Revised:
31 December 2015

Accepted:
18 January 2016

doi: 10.1259/bjr.20150980

Cite this article as:
Keraliya AR, Krajewski KM, Jagannathan JP, Shinagare AB, Braschi-Amirfarzan M, Tirumani SH, et al. Multimodality imaging of osseous involvement In haematological malignancies. *Br J Radiol* 2016; **89**: 20150980.

REVIEW ARTICLE

Multimodality imaging of osseous involvement In haematological malignancies

[1,2]ABHISHEK R KERALIYA, MBBS, MD, [1,2]KATHERINE M KRAJEWSKI, MD, [1,2]JYOTHI P JAGANNATHAN, MD, [1,2]ATUL B SHINAGARE, MD, [1,2]MARTA BRASCHI-AMIRFARZAN, MD, [1,2]SREE H TIRUMANI, MD and [1,2]NIKHIL H RAMAIYA, MD

[1]Department of Imaging, Dana Farber Cancer Institute, Harvard Medical School, Boston, MA
[2]Department of Radiology, Brigham and Women's Hospital, Harvard Medical School, Boston, MA

Address correspondence to: Dr Abhishek R Keraliya
E-mail: *akeraliya@partners.org*

ABSTRACT

The purpose of this article is to provide a comprehensive review of the imaging features of osseous involvement in haematological malignancies. Osseous involvement can be seen in various haematological malignancies including lymphomas, plasma cell neoplasms, leukaemias and myeloproliferative neoplasms. Imaging plays a crucial role in initial diagnosis, staging and in the assessment of treatment response in these patients.

INTRODUCTION

Haematological malignancies can be broadly divided into the lymphomas, plasma cell neoplasms, leukaemias, myeloproliferative neoplasms, histiocytic and dendritic cell neoplasms.[1] Osseous involvement in haematological neoplasms may be confined to the bone marrow or involve the cortical and cancellous bone. Various imaging modalities including conventional radiography, CT, bone scintigraphy, PET/CT and MRI are useful in initial diagnosis and treatment response assessment of osseous involvement in various haematological malignancies. In this article, we present a comprehensive review of the spectrum of imaging findings of osseous involvement in common haematological malignancies.

ROLE OF IMAGING

Conventional radiography is the first-order diagnostic study and most cost-effective means for the assessment of the cortical and trabecular bone; however, it is not suitable for evaluation of the bone marrow, which is the primary site of involvement in haematological malignancies. Moreover, a change of 30–50% in mineral density is needed before a bone lesion becomes apparent on radiographs. CT has higher sensitivity than plain radiography in detecting small lytic lesions and identifying subtle fractures. CT is also useful for displaying cortical disruption, periosteal reaction and soft tissue involvement. Limitations of CT include relatively high radiation exposure and relative insensitivity in detecting subtle marrow changes. Bone scintigraphy is highly sensitive method of detecting osteoblastic response seen in various osseous pathologies.[2] Technetium-99m-labelled methylene diphosphonate bone scintigraphy is useful in confirming the presence of disease and demonstrating the distribution of disease in the skeleton. The major limitations of bone scintigraphy are the lack of specificity and relative insensitivity in detecting lytic osseous lesions, such as in multiple myeloma. Fluorine-18 fludeoxyglucose positron emission tomography (^{18}F-FDG PET)/CT is a functional imaging technique which is useful in diagnosing focal osseous lesions as well as in detecting diffuse bone marrow involvement. PET/CT is useful as a one-stop shop modality, providing a whole-body (WB) evaluation in one session and its utility in evaluating treatment response.

MRI is the modality of choice for non-invasive evaluation of various marrow disorders because of its superior contrast resolution and ability to differentiate haematopoietic and fatty marrow. High-sensitivity, WB imaging capability and lack of ionizing radiation make MRI the preferred modality for bone marrow imaging. Commonly used MRI sequences for bone and marrow imaging include T_1 weighted (T1W), T_2 weighted (T2W), proton density and diffusion-weighted imaging (DWI) sequences and, when indicated, T1W images after intravenous application of contrast agent (gadolinium). T2W images are usually combined with a fat saturation technique such as short tau inversion recovery (STIR). T1W images provide excellent

Table 1. Staging systems for multiple myeloma

Stage	Durie-Salmon staging system	International staging system
I	• Haemoglobin value $>10\,g\,dl^{-1}$ • Normal serum calcium • Bone radiography: normal bone structure or solitary bone plasmacytoma only • Low levels of M protein in the blood or urine	• Serum β2-microglobulin $<3.5\,mg\,l^{-1}$ • Serum albumin $\geq 3.5\,g\,dl^{-1}$
II	Not Stage I or III	Not Stage I or III
III	One or more of the following: • Haemoglobin value $<8.5\,g\,dl^{-1}$ • Serum calcium $>12\,mg\,dl^{-1}$ • Advanced lytic bone lesions • High M-component production rate	Serum β2-microglobulin $\geq 5.5\,mg\,l^{-1}$

anatomical detail with high specificity for abnormalities of the bone marrow. T2W images are usually combined with a fat saturation technique to demonstrate increased water content within the bone marrow and soft tissues. STIR is generally used with larger fields of view and is highly sensitive for the detection of marrow oedema. DWI is also helpful in evaluation of various marrow infiltrative disorders. DWI is a functional MRI technique that depicts differences in the mobility of water in tissues. The corresponding apparent diffusion coefficient quantifies the mobility of water protons in tissues. Neoplasms exhibit more restricted water diffusion than normal tissues, which is reflected as high signal intensity on DWI.

MR APPEARANCE OF NORMAL BONE MARROW AND HOW TO DIFFERENTIATE BETWEEN INFILTRATIVE PATHOLOGY FROM NORMAL HAEMATOPOIETIC MARROW

The medullary cavity of bones contains three components: red (haematopoietic) marrow, yellow (non-haematopoietic) marrow and trabecular bone in different proportions according to the type of bone and the age of the person. The bone marrow is a dynamic organ that changes composition throughout life. At birth, the bone marrow is predominantly composed of haematopoietically active cells. As the individual ages, there is predictable conversion of haematopoietic to fatty marrow. The marrow conversion process begins in the appendicular skeleton and progresses to the axial skeleton.[3] In long bones, marrow conversion starts in the mid diaphysis and epiphysis, then progresses to distal metaphysis and finally to proximal metaphysis. In adults, the red marrow is distributed in the axial skeleton and the proximal aspects of the limbs. Generally, the distribution of marrow infiltrative disease is dependent on the distribution of the red marrow because of its rich blood supply as compared with fatty marrow.

The MRI appearance of the bone marrow depends on the presence and relative proportions of water, fat and trabecular bone.[4] Owing to short T_1 relaxation time of fat protons, the yellow marrow displays high signal intensity on T1W sequences, nearly similar to that of subcutaneous fat. In adults, long bones typically show high T_1 signal intensity owing to predominantly fatty marrow. T_1 signal intensity of the red marrow is lower than that of the yellow marrow owing to its higher cellularity and low fat content, however showing higher signal intensity than that of the muscles. Using skeletal muscle as an internal standard, it is possible to differentiate between infiltrative pathology (isointense or hypointense to muscle) from normal haematopoietic marrow (hyperintense compared with muscles) on T1W spin-echo MRI. For evaluation of the spine, the intervertebral disc may serve as the internal standard for differentiating infiltrative pathology from normal haematopoietic marrow, with the latter being hyperintense compared with the disc on T1W images.[5]

On T2W spin-echo sequences, the fatty marrow has higher signal intensity than the muscle. On fat-saturated or STIR images, haematopoietic marrow shows intermediate signal intensity, similar to that of muscles, whereas the fatty marrow shows more hypointense signal.[3,4] Most of the neoplasms and pathological marrow infiltrative disorders are typically hyperintense to red or yellow marrow on STIR images owing to the high water content of the neoplastic cells. After gadolinium administration, normal marrow enhancement in healthy persons can vary greatly and is dependent on age, however is significantly lower than pathological marrow infiltration.[6]

PLASMA CELL NEOPLASMS

Plasma cell neoplasms arise from mature B lymphocytes and include multiple myeloma, plasmacytoma and Waldenström macroglobulinaemia (WM). Monoclonal gammopathy of unknown significance (MGUS) and smouldering multiple myeloma are asymptomatic plasma cell dyscrasias, which can

Table 2. Durie-Salmon plus staging system

Classification	MRI and/or ^{18}F-FDG PET findings
I	<5 focal lesions; mild diffuse disease
II	5–20 focal lesions; moderate diffuse disease
III	>20 focal lesions; severe diffuse disease

^{18}F-FDG, fluorine-18 fludeoxyglucose; PET, positron emission tomography.

Figure 1. A 60-year-old female with multiple myeloma. (a) Plain radiograph of the skull (lateral view) demonstrating multiple lytic lesions. (b) Axial T_1 weighted MR image showing an expansile lesion involving right parietal bone with extraosseous soft-tissue component (arrow). The lesion shows hypointense signal compared with that of fatty marrow of the diploic cavity.

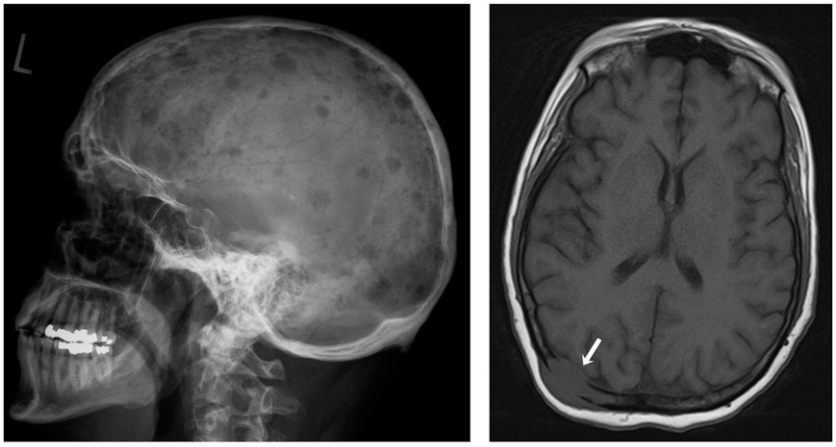

(a) (b)

progress to multiple myeloma. MGUS is the most common asymptomatic plasma cell dyscrasia with prevalence of >3% in populations more than 50 years of age and has an average multiple myeloma progression risk of 1% per year.[7] Smouldering myeloma is a heterogeneous clinical entity that mimics MGUS and has more indolent course of disease than multiple myeloma. It is defined as either serum M-protein $\geq 3\,g\,l^{-1}$ or ≥10% monoclonal plasma cells in the bone marrow with no myeloma-related organ or tissue impairment.[8]

Multiple myeloma is the most common primary malignant bone neoplasm in adults. The majority of patients with multiple myeloma and plasmacytoma are more than 60 years of age at presentation with increasing incidence with age. The median age at diagnosis is 66 years; with a male predominance.[9] Multiple myeloma occurs due to an uncontrolled proliferation of a single clone of differentiated plasma cells in the bone marrow. It is characterized by the presence of monoclonal immunoglobulins in the serum and/or urine, although approximately 3% of patients have no M-protein in the serum or urine (non-secretory myeloma). Patients present with a variety of signs and symptoms (anaemia, bone pain, fatigue, hypercalcaemia, elevated creatinine and weight loss) owing to plasma cell infiltration of the bone or other organs or owing to kidney damage from excess light chains.[9]

In patients with multiple myeloma, uncontrolled proliferation of plasma cells occurs primarily within the marrow space resulting in skeletal destruction with osteolytic lesions, osteopenia and/or pathological fractures. Myeloma lesions closely follow the red marrow distribution pattern and mostly involve the axial skeleton (skull, spine, rib cage and pelvis) and proximal appendicular skeleton. Osseous destruction represents a major cause of morbidity and mortality in myeloma patients and manifests as severe bone pain, pathological fractures, spinal cord compression and hypercalcaemia. A plasmacytoma is a discrete, solitary mass of neoplastic plasma cells in either the bone or soft tissue. Solitary plasmacytomas most frequently occur in the bone but can also be found in soft tissues (extramedullary plasmacytoma). The most common location of solitary plasmacytoma is within a vertebral body. The thoracic vertebrae are most commonly involved, followed by the lumbar, sacral and cervical vertebrae.

Figure 2. A 65-year-old female with multiple myeloma. (a) Sagittal T_1 weighted (T1W) MR image of lumbosacral spine showing bone marrow infiltration characterized by diffuse marrow hypointensity. (b) Sagittal contrast-enhanced T1W image showing diffuse heterogeneous marrow enhancement involving lumbosacral spine.

(a) (b)

Figure 3. A 43-year-old female with multiple myeloma. (a, b) Pre-treament sagittal T_1 weighted (T1W) (a) and T_2 weighted (T2W) (b) MR images of the cervical spine showing marrow involvement of the C5 vertebra with pre-vertebral (arrows) and anterior epidural (arrowhead) soft-tissue components (b). Post-treatment sagittal post-contrast T1W (c) and T2W (d) MR images showing hypointense marrow signal of the affected C5 vertebra (arrows) with resolution of soft-tissue component.

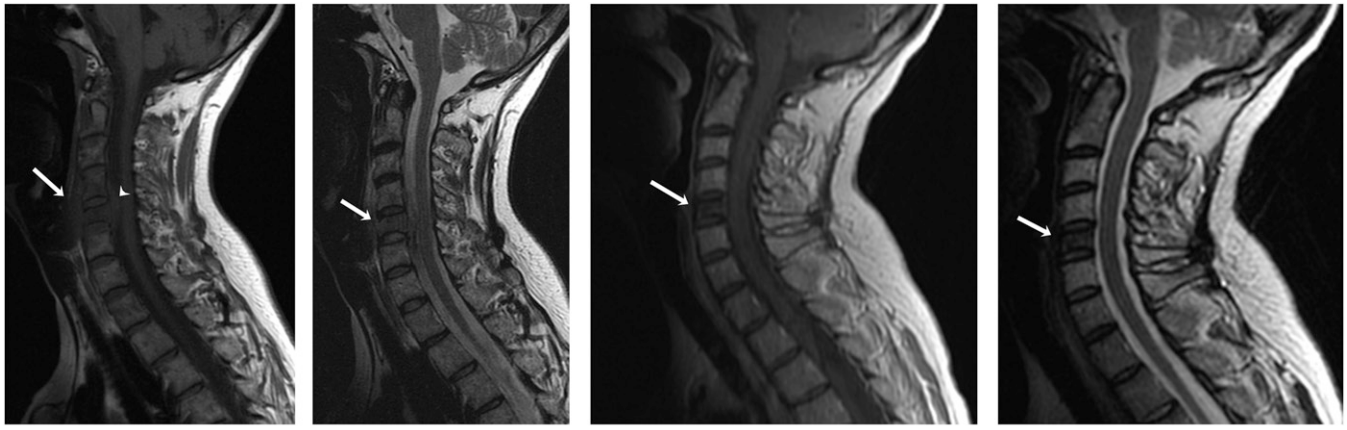

The main role of imaging in multiple myeloma is in initial staging of the disease, detection and characterization of complications and in the evaluation of treatment response. According to the International Myeloma Working Group in 2009 and International Myeloma Consensus Panels in 2011, conventional radiography remains the standard method for imaging screening in patients with multiple myeloma; however, newer imaging modalities, such as MRI, CT and ^{18}F-FDG PET/CT, are frequently used for better diagnostic and prognostic evaluation.[10,11] Multiple myeloma is widely staged using the Durie-Salmon system which divides myeloma into three stages based on four factors haematocrit, serum calcium, amount of abnormal monoclonal immunoglobulin in the blood or urine and the presence and number of bony lesions on radiographs (Table 1).[12] In 2006, the Durie-Salmon PLUS staging system was proposed to include lesions seen with ^{18}F-FDG PET/CT and MRI to evaluate the extent and severity of multiple myeloma (Table 2).[13] Alternate staging systems for multiple myeloma include the International Staging System which defines three risk groups on the basis of serum β-microglobulin and albumin levels.[14]

Typical appearance of myeloma on radiography is punched-out lesions without reactive surrounding sclerosis in the skull, spine and pelvic bones (Figure 1a). Generalized osteopenia may be the only osseous manifestation of myeloma in up to 15% of patients. Other patterns of skeletal involvement are described in the literature and include solitary plasmacytoma or rarely osteosclerosing myeloma.[15,16] Thinning of the inner cortical bone (scalloping) and multiple small lesions producing a "moth-eaten" appearance can also be seen. In the skull, diffuse lytic lesions of myeloma give rise to the classic "pepper pot skull". A major disadvantage of conventional radiography in diagnosis and staging of patients with myeloma is limited sensitivity, as radiographs reveal lytic disease only when >30% of the trabecular bone has been lost.[17] CT has higher sensitivity than conventional radiography in detecting small lytic bony lesions. CT is also helpful for evaluation of extraosseous lesions and for image-guided biopsy.[18] Bone scintigraphy is of limited value in multiple myeloma owing to the lack of osteoblastic activity.

Figure 4. A 68-year-old female with multiple myeloma. Coronal short tau inversion recovery whole-body MR image showing compression fractures involving the L3 and L5 vertebrae (arrows) with hyperintense marrow signal suggestive of oedema.

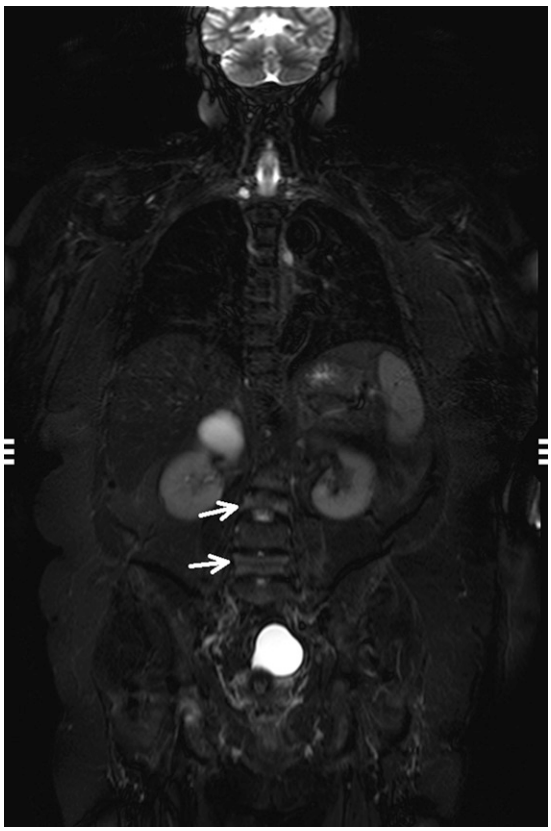

Figure 5. A 62-year-old female with multiple myeloma. (a) Anteroposterior radiograph of the right humerus demonstrates a lytic diaphyseal lesion (arrow). (b) Follow-up radiograph 1 year after stem cell transplantation shows appearance of peripheral sclerosis around the lytic lesion (arrow).

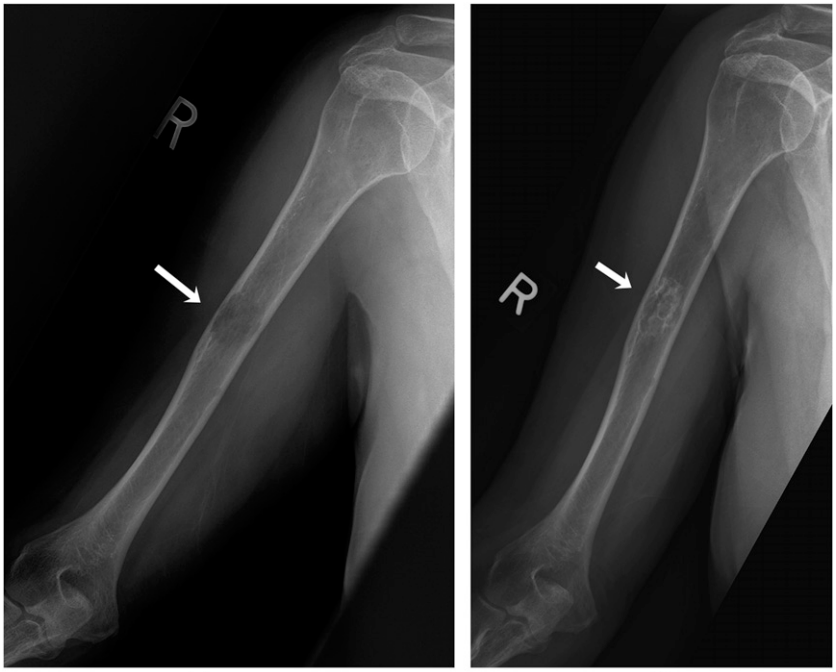

MRI is particularly useful in evaluation of extraskeletal soft-tissue masses adjacent to the bone and better visualization of marrow involvement. MRI has higher sensitivity than radiographs, CT and bone scintigraphy. MRI has the advantage of sensitivity for the presence of disease and superior soft tissue contrast resolution; however, its specificity is limited. Typical myeloma lesions involve the bone marrow and have low signal intensity on T1W images (Figure 1B) and high signal intensity on T2W and STIR sequences. MR patterns of bone marrow involvement are classified as homogeneous diffuse bone marrow infiltration, focal lesions, mixed pattern with focal lesions on the background of diffuse abnormality and normal appearance of the bone marrow with microscopic plasma cell infiltration (Figure 2).[19,20] According to a study of 28 patients with extramedullary myeloma, the majority of the lesions are hypointense to isointense on T1W images and isointense to hyperintense on T2W images compared with the skeletal muscles.[21] The post-treatment appearance of marrow lesions varies in MRI and includes resolution of marrow abnormality or persistent abnormality without enhancement or with peripheral rim enhancement.[22] Replacement of infiltrated marrow by fat may manifest as hyperintense signal on T1W images, whereas sclerotic healing response manifests as reduction in T1 and T2 signal intensities (Figure 3). WB MRI is increasingly used for the initial assessment of myeloma.[23] According to a study of 24 patients with bone marrow biopsy-proven multiple myeloma, WB MRI had a higher sensitivity and specificity than PET in the assessment of disease activity[24] (Figure 4). MRI is also useful in predicting the prognosis in patients with multiple myeloma. According to a study of 113 patients with newly diagnosed multiple myeloma, spine MRI at the time of diagnosis was found useful in detecting malignancy-associated compression fractures and extramedullary myeloma, including epidural extension of the tumour.[25] Furthermore, extramedullary plasmacytoma was associated with poor overall survival.

In recent years, ^{18}F-FDG PET/CT has emerged as a powerful diagnostic tool for evaluation of patients with myeloma; ^{18}F-FDG PET/CT is used as initial imaging to identify the presence of additional osseous and extraosseous lesions in patients with solitary plasmacytoma of bone. PET/CT and MRI are particularly useful in the detection of extraosseous manifestations of multiple myeloma, which can affect various organ systems including the lymph nodes, central nervous system, skeletal muscles, lungs, liver, pancreas, adrenal and subcutaneous tissues.[21] PET/CT is also valuable in assessing prognosis and therapeutic response in patients with myeloma. According to a single-centre study of 239 untreated patients, the presence of more than three ^{18}F-FDG -avid focal lesions is positively linked to high levels of beta-2-microglobulin, C-reactive protein and lactate dehydrogenase and is associated with inferior overall and event-free survival.[26] PET/CT has higher specificity for evaluation of therapeutic response than MRI, on which signal abnormalities persist years after treatment.[27] Response criteria specific to osseous metastases have been developed at the University of Texas MD Anderson Cancer Center.[28] On radiographs and CT, response may be indicated by the appearance of a sclerotic rim around the lytic osseous lesions (Figure 5). On MRI, peripheral T_1 hyperintensity around a previously hypointense lesion can suggest treatment response.

Figure 6. A 43-year-old female with Waldenström macroglobulinaemia. (a) Coronal-fused fluorine-18 fludeoxyglucose positron emission tomography (^{18}F-FDG PET)/CT image shows ^{18}F-FDG-avid bilateral axillary lymphadenopathy (black arrows), splenic involvement (white arrow) and diffuse skeletal uptake (white arrowheads) consistent with bone marrow involvement. (b) Post-treatment coronal fused ^{18}F-FDG PET/CT image shows significant interval decrease in ^{18}F-FDG-avid disease involving spleen (white arrow) and bone marrow (white arrowheads).

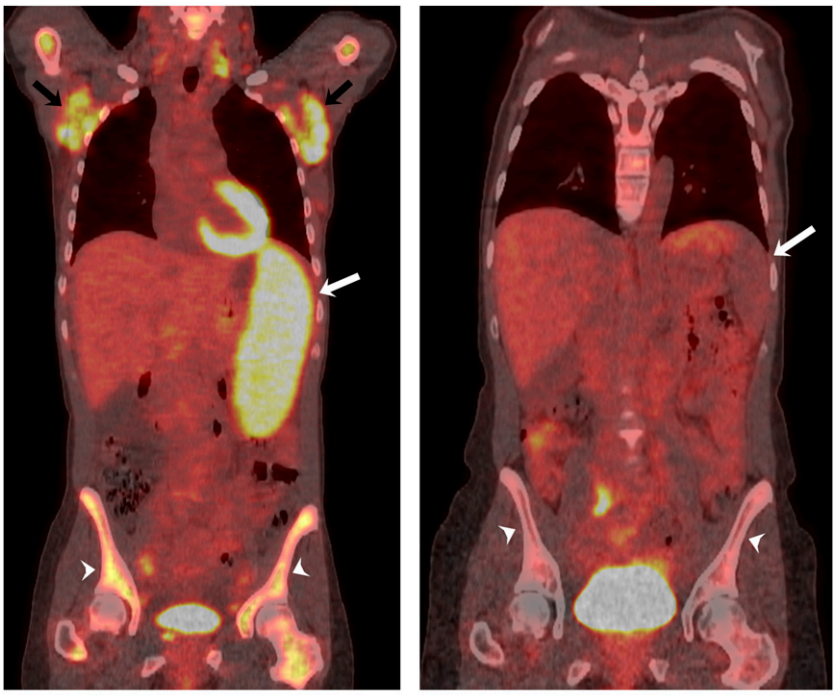

(a) (b)

Waldenström macroglobulinaemia

WM, also known as lymphoplasmacytic lymphoma, is a distinct lymphoproliferative disorder of B-cell origin characterized by immunoglobulin M monoclonal gammopathy in the blood and lymphoplasmacytic cells in the bone marrow. Patients with WM usually present with cytopenias, hyperviscosity, neuropathy, hepatosplenomegaly and lymphadenopathy.[29] Focal osseous lesions are rarely seen on conventional radiographs in patients with WM. MRI and ^{18}F-FDG PET/CT are useful imaging modalities to assess bone marrow involvement in patients with WM. According to a single-centre study of 23 consecutive patients, MRI identified marrow abnormalities in 90% of patients with WM.[30] Two types of imaging patterns were classified. The diffuse pattern manifests as isointense or hypointense marrow signal compared with the adjacent muscle on T1W images. The other pattern with variegated involvement shows innumerable tiny foci of marrow replacement scattered throughout the marrow.[30] ^{18}F-FDG PET/CT has sensitivity of >80% in detecting disease involvement, including bone marrow involvement in patients with WM compared with CT alone (43% *vs* 8%).[31] Also in the same study, ^{18}F-FDG PET/CT was found to be more sensitive in treatment response assessment than CT (Figure 6).

Lymphoma

The lymphoproliferative disorders are classified into Hodgkin's lymphoma (HL) and non-HL (NHL). Osseous involvement in lymphoma can be primary (without any supraregional lymph node involvement or other extranodal lesion) or secondary.[32] Secondary osseous involvement in lymphoma may occur as a part of disseminated disease or in relapsed disease with involvement of the bone. Secondary osseous lymphoma is indistinguishable from primary lymphoma of the bone (PLB) on immunocytological analysis, and imaging findings in primary and secondary lymphoma of the bone are similar.

Primary lymphoma of the bone

PLB is a rare manifestation of HL and NHL, accounting for <5% of bone tumours and <2% of lymphomas.[33] The majority of them are usually large B-cell-type NHL, with diffuse large B-cell lymphoma being the most common histological subtype.[32] Rarely, indolent lymphomas (follicular lymphoma, marginal zone lymphoma and small lymphocytic lymphoma) may present as PLB. Highly aggressive lymphoma subtypes, such as Burkitt lymphoma, anaplastic large-cell lymphoma and lymphoblastic lymphoma can also have osseous involvement. HL accounts for <10% of PLB.[34] Although PLB can occur at any age, >50% of cases occur in patients over the age of 60 years, with slight male predominance.[35] PLB occurs more commonly in the axial skeleton than in the appendicular skeleton.

Conventional radiographs, CT and MRI are the commonly used modalities for PLB. ^{18}F-FDG -PET/CT is useful to exclude occult systemic lymphoma. Lymphoma can involve bone marrow, cortex and also may have extraosseous soft tissue involvement. The radiographic features of osseous lymphoma are variable and the pattern can be normal, predominantly lytic, sclerotic or mixed lytic–sclerotic.[36] The typical imaging appearance of PLB

Figure 7. A 80-year-old female with primary B-cell non-Hodgkin's lymphoma involving the right distal femur. (a) Lateral radiograph of the right femur shows ill-defined lytic lesion involving distal femoral metaphysis with cortical destruction (arrow). (b) Coronal T_1 weighted MR image shows low signal intensity of the tumour relative to fatty marrow of the epiphysis and periosteal reaction and soft tissue (arrows).

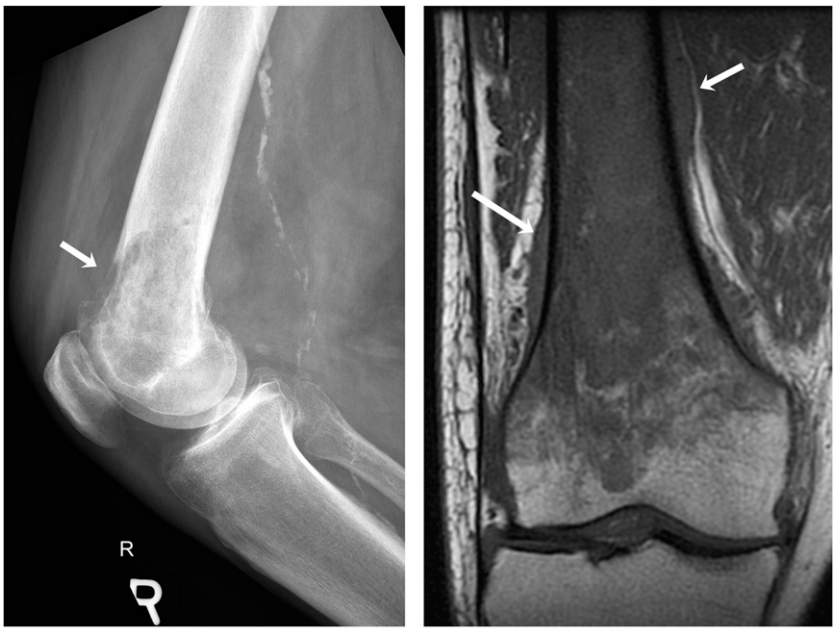

on conventional radiographs is that of a lytic (70%) or mixed-density (28%) lesion with a permeative or moth-eaten pattern (Figure 7A).[34] Diffuse medullary mottling is usually the first radiographic sign. Relative absence of cortical destruction favours lymphoma over other bony neoplasms. Associated lamellated or sunburst periosteal reaction with cortical destruction can occur. Sequestra are seen in approximately 10% of PLB.[37] CT is superior to conventional radiography in the detection of cortical and trabecular destruction, periosteal reaction, sequestrum and extraosseous extension. Approximately half of the lesions have an associated soft-tissue mass.[34] CT and MRI are more sensitive in identifying soft tissue involvement associated with PLB than radiographs. On MRI, PLB demonstrates low signal intensity compared with normal bone marrow on T1W images (Figure 7B). However, on T2W sequences, PLB has more heterogeneous appearance with variable signal intensity ranging from hypointense, isointense or hyperintense relative to fat.[38,39]

Secondary osseous involvement

Bone marrow infiltration is categorized as an extranodal site in staging of lymphoma and is associated with a poor prognosis in newly diagnosed patients with lymphoma. Up to 40% of patients with NHL have disseminated disease with extranodal involvement at presentation, including bone marrow involvement.[40] Secondary osseous involvement occurs in 5–20% of patients during the course of Hodgkin's disease (Figure 8). Most osseous lymphomatous involvement results from contiguous nodal or haematogenous spread. Vertebral lesions occur

Figure 8. A 26-year-old male with relapsed Hodgkin's lymphoma and osseous involvement. (a) Axial CT image of the the pelvis in bone window settings demonstrates sclerosis of the right acetabulum (arrow) with periosteal reaction (arrowheads). (b) Coronal short tau inversion recovery MR image shows marrow hyperintensity involving the right iliac bone and acetabulum along with periosteal reaction (arrow).

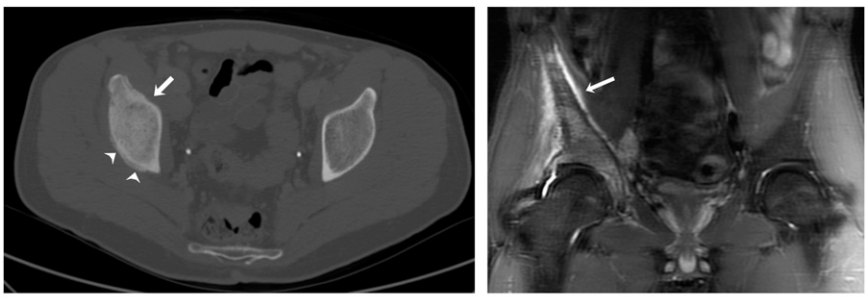

Figure 9. A 65-year-old female with diffuse large B-cell lymphoma. (a) Axial T_2 weighted (b) MR image showing heterogeneous expansile lesion involving the clivus (arrow). (b) Axial contrast-enhanced T_1 weighted MR image showing heterogeneous enhancement of the lesion (arrow) with encasement of cavernous segment of internal carotid arteries on both sides (arrowheads).

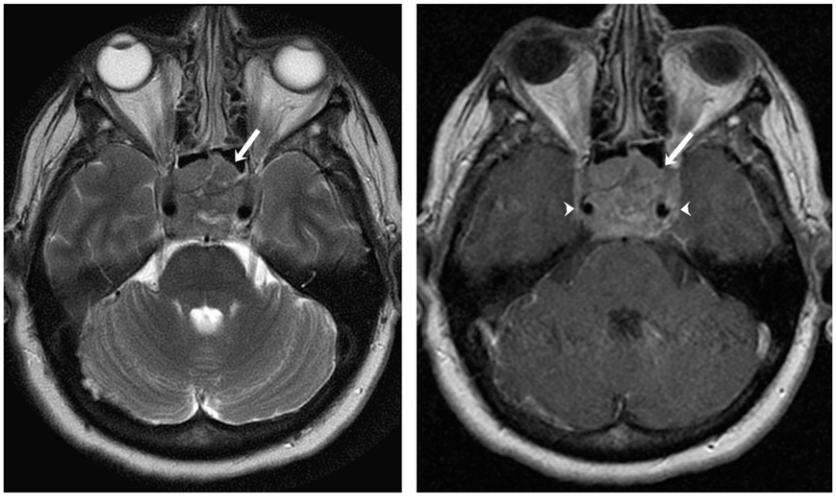

(a) (b)

most frequently in the thoracic and lumbar spine. Lytic lesions are more common but patchy sclerosis and classic "ivory vertebrae" are frequently seen.[41] Associated extraosseous soft-tissue masses and pathological collapse are also common.

MRI is particularly useful in the evaluation of lymphomatous bone marrow involvement, which can be multifocal or diffuse. Lymphomatous bone marrow lesions typically have low signal intensity on T1W images and high signal intensity on fat-saturated T2W or STIR sequences with moderate to marked contrast enhancement (Figure 9). One characteristic finding of lymphoma is restricted diffusion with low apparent diffusion coefficient values on DWI due to hypercellularity. Extraosseous extension of tumour without cortical destruction is well demonstrated on MRI (Figure 10). With recent technical advances in MRI, WB MRI is becoming a promising tool and viable alternative to PET/CT for the diagnosis and staging of bone marrow involvement of lymphoma, particularly in paediatric and pregnant patients, without using ionizing radiation or an intravenous contrast agent.[42] According to recent studies, DWI-MRI has high sensitivity up to 97% compared with PET/CT for staging, follow-up and treatment response assessment in patients with ^{18}F-FDG -avid lymphoma.[43,44] WB diffusion-weighted MRI is usually well tolerated by patients owing to the relatively shorter acquisition time, which is typically shorter than that for PET/CT.

Numerous studies have validated and confirmed the utility of ^{18}F-FDG PET for staging as well as interim and end-of-therapy treatment response assessment of lymphoma. In recent years, many studies have shown the usefulness of ^{18}F-FDG PET/CT for diagnosis of bone/bone marrow lesions in both HL and

Figure 10. A 22-year-old male with Burkitt's lymphoma. (a). Sagittal T_1 weighted (T1W) MR image showing T_1 hypointensity involving the frontal bone with associated extradural (arrowheads) and scalp soft-tissue mass (arrow). (b) Coronal T1W MR image shows hypointense lesion involving the distal end of the femur (arrow).

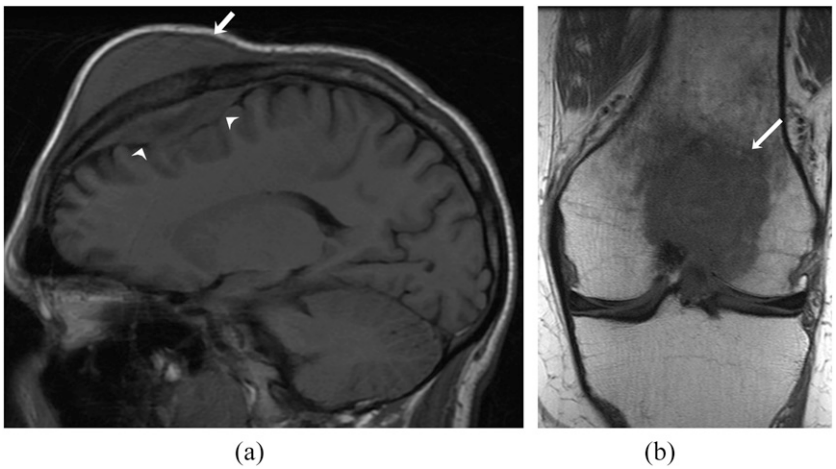

(a) (b)

Figure 11. A 45-year-old male with chronic myeloid leukaemia and multiple myeloid sarcoma. (a) Anteroposterior radiograph of the right femur shows no significant abnormality. (b) Coronal T_1 weighted MR image shows large T_1 hypointense lesions in the distal femur and proximal tibia (arrows) and numerous other ill-defined smaller lesions.

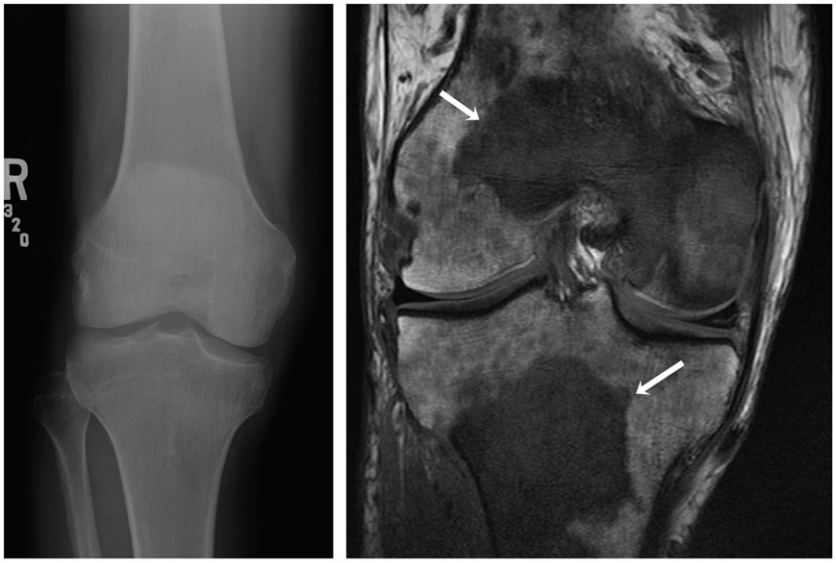

NHL.[45–47] In a retrospective study of 122 newly diagnosed biopsy-proven cases of HL, Muzahir et al[48] found the sensitivity of ^{18}F-FDG PET/CT is nearly 100% with the specificity of 76.57% compared with bone marrow biopsy. Similarly in NHL patients, PET/CT has better diagnostic performance and prognostic stratification than bone marrow biopsy. In a single-institution retrospective study of 133 patients with newly diagnosed diffuse large B-cell lymphoma, ^{18}F-FDG PET/CT had higher sensitivity (94%), negative-predictive value (98%) and accuracy (98%) compared with bone marrow sampling (24%, 80%, 81%, respectively).[49] ^{18}F-FDG PET/CT and bone marrow biopsy have a high concordance rate (80%) for detecting bone marrow involvement.[50] In evaluation of treatment response in patients with lymphoma, PET/CT is now widely accepted as one of the most accurate non-invasive modalities. As functional changes usually precede morphological changes after treatment, ^{18}F-FDG PET/CT is better for the evaluation of treatment response, as ^{18}F-FDG uptake decreases before morphological changes become evident on conventional radiography, CT or MRI.

LEUKAEMIA AND MYELOID SARCOMA

Leukaemia refers to a group of haematopoietic neoplasms involving myeloid or lymphoid cell lineage of the bone marrow. Leukaemia is the most common childhood malignancy, and musculoskeletal manifestations symptoms can be seen in up to 40% patients with acute leukaemia.[51] Various radiographic abnormalities in patients with leukaemia include osteoporosis,

Figure 12. A 57-year-old male with primary myelofibrosis. (a) Coronal T_1 weighted MR image demonstrates diffuse marrow infiltration involving both distal femurs (arrows). (b) Coronal contrast-enhanced CT image in bone window settings shows splenomegaly (arrow) with diffuse osteosclerosis.

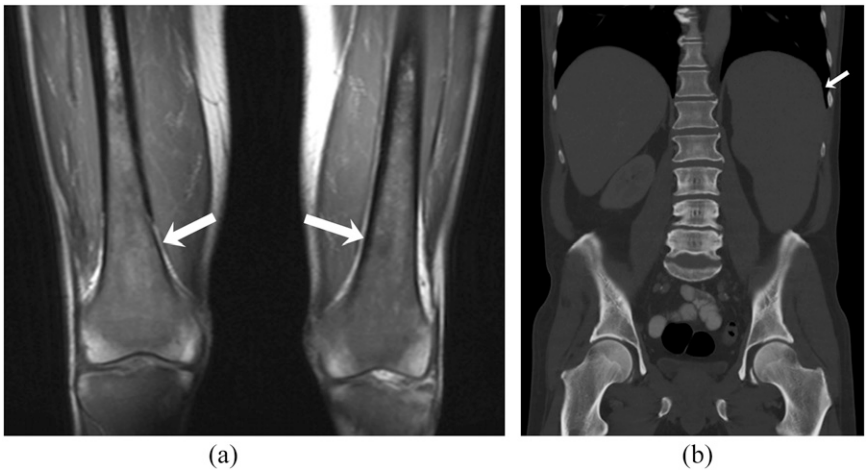

pathological fractures, metaphyseal bands, pathological fractures, osteosclerosis and periosteal reaction.[51,52] Marrow infiltration by leukaemic cells is typically diffuse with replacement of red or yellow bone marrow cells, resulting in a diffuse decrease in marrow signal intensity on T1W MR images.

Myeloid sarcoma, also known as chloroma and granulocytic sarcoma, is a solid extramedullary neoplasm composed of primitive myeloid cells, which occur in patients with myeloproliferative disorders, especially in acute myeloid leukaemia.[53] Myeloid sarcoma may occur in patients with acute myeloid leukaemia, myelodysplastic syndrome, myeloproliferative neoplasm, essential thrombocythaemia and polycythaemia vera. It can occur as the initial symptom of the underlying haematologic malignancy or be the first sign of relapse in patients previously treated for primary or secondary acute leukaemia. Myeloid sarcoma presents during remission of underlying haematologic disorder in up to 80% of patients.[54] Myeloid sarcoma may be the first manifestation of blastic transformation in patients with myelodysplastic syndrome or myeloproliferative neoplasm. Occasionally, myeloid sarcoma may occur *de novo* in healthy persons in the absence of underlying haematologic malignancy or precede the systemic malignancy by months or years.

Osseous involvement is seen in approximately 50% of patients with myeloid sarcoma, and the spine, pelvis and lower extremity bones are commonly involved.[54] Imaging characteristics of osseous myeloid sarcoma is similar to that of other marrow neoplastic disorders, typically hypointense on T1W images and mildly hyperintense on T2W images compared with skeletal muscles and usually shows homogeneous enhancement greater than that of muscle on contrast-enhanced T1W images (Figure 11). ^{18}F-FDG PET/CT is useful in detection of additional clinically occult disease sites, staging and monitoring the response to treatment.[55]

Myelofibrosis

Myelofibrosis is often primary but may be secondary to a number of malignant and non-malignant conditions. Primary myelofibrosis (PMF) is a chronic myeloproliferative neoplasm of unknown origin characterized by progressive bone marrow fibrosis. PMF is a clonal proliferation of a pluripotent haemopoietic stem cell causing production of cytokines such as fibroblast growth factor leading to replacement of the haematopoietic bone marrow by collagen fibers.[56] PMF usually affects elderly patients with a peak incidence between 50 and 70 years of age.[57] Patients present with anaemia, malaise, weight loss, fever or symptoms due to splenic enlargement.[56] Marked splenomegaly is a frequent manifestation of myelofibrosis (Figure 12).[58]

Myelofibrosis is characterized by a number of radiological changes as a result of marrow fibrosis and extramedullary haematopoiesis. The primary osseous imaging finding in patients with myelofibrosis is diffuse osteosclerosis involving the axial skeleton, ribs and proximal humerus and femur (Figure 10). Purely osteolytic lesions are extremely rare.[59] Also, periostitis occurs in few patients with myelofibrosis, seen on radiographs as periosteal new bone formation in extremities.[60] Other imaging manifestations in patients with myelofibrosis include hepatosplenomegaly, lymphadenopathy and extramedullary haematopoiesis in other organ systems.[61] In the spine, two different patterns of osteosclerosis can be seen: a diffuse homogeneous pattern or involvement of the superior and inferior margins of the vertebral body (sandwich vertebrae).[62]

On MRI, bone marrow in patients with myelofibrosis shows low intensity on both T1W and T2W images (Figure 12).[62] On ^{18}F-FDG PET/CT, myelofibrosis is characterized by diffusely increased uptake throughout the bone marrow.[63] Owing to increased cortical blood flow in myelofibrosis, bone scintigraphy demonstrates diffusely increased activity in all bones resulting in a "superscan" phenomenon.[64]

CONCLUSION

Osseous involvement can be seen in various haematological malignancies including lymphoma, plasma cell neoplasms, leukaemia and myeloproliferative neoplasms. Imaging plays a crucial role in the initial diagnosis and staging of the disease in these patients. Knowledge about normal physiological marrow conversion and difference in signal intensity on T1W MRI helps in differentiation between infiltrative pathology from normal haematopoietic marrow. ^{18}F-FDG PET/CT, being a functional imaging modality, is particularly important in predicting prognosis and detecting early treatment response.

REFERENCES

1. Swerdlow SH, Campo E, Harris NL, Jaffe ES, Pileri SA, Stein H, et al: *WHO Classification of tumours of haematopoietic and lymphoid tissues*, 4th edn; 2008.
2. Malmud LS, Charkes ND. Bone scanning: principles, technique and interpretation. *Clin Orthop Relat Res* 1975; (107): 112–22. doi: http://dx.doi.org/10.1097/00003086-197503000-00013
3. Vogler JB 3rd, Murphy WA. Bone marrow imaging. *Radiology* 1988; **168**: 679–93. doi: http://dx.doi.org/10.1148/radiology.168.3.3043546
4. Vande Berg BC, Malghem J, Lecouvet FE, Maldague B. Magnetic resonance imaging of the normal bone marrow. *Skeletal Radiol* 1998; **27**: 471–83. doi: http://dx.doi.org/10.1007/s002560050423
5. Carroll KW, Feller JF, Tirman PF. Useful internal standards for distinguishing infiltrative marrow pathology from hematopoietic marrow at MRI. *J Magn Reson Imaging* 1997; **7**: 394–8. doi: http://dx.doi.org/10.1002/jmri.1880070224
6. Baur A, Stäbler A, Bartl R, Lamerz R, Scheidler J, Reiser M. MRI gadolinium enhancement of bone marrow: age-related changes in normals and in diffuse neoplastic infiltration. *Skeletal Radiol* 1997; **26**: 414–18. doi: http://dx.doi.org/10.1007/s002560050257
7. Kyle RA, Therneau TM, Rajkumar SV, Larson DR, Plevak MF, Offord JR, et al. Prevalence of monoclonal gammopathy of undetermined significance. *N Engl J Med* 2006; **354**: 1362–9. doi: http://dx.doi.org/10.1056/NEJMoa054494
8. Korde N, Kristinsson SY, Landgren O. Monoclonal gammopathy of undetermined

significance (MGUS) and smoldering multiple myeloma (SMM): novel biological insights and development of early treatment strategies. *Blood* 2011; **117**: 5573–81. doi: http://dx.doi.org/10.1182/blood-2011-01-270140
9. Kyle RA, Gertz MA, Witzig TE, Lust JA, Lacy MQ, Dispenzieri A, et al. Review of 1027 patients with newly diagnosed multiple myeloma. *Mayo Clin Proc* 2003; **78**: 21–33. doi: http://dx.doi.org/10.4065/78.1.21
10. Dimopoulos M, Terpos E, Comenzo RL, Tosi P, Beksac M, Sezer O, et al; Imwg. International myeloma working group consensus statement and guidelines regarding the current role of imaging techniques in the diagnosis and monitoring of multiple Myeloma. *Leukemia* 2009; **23**: 1545–56. doi: http://dx.doi.org/10.1038/leu.2009.89
11. Dimopoulos M, Kyle R, Fermand JP, Rajkumar SV, San Miguel J, Chanan-Khan A; International Myeloma Workshop Consensus Panel 3. Consensus recommendations for standard investigative workup: report of the International Myeloma Workshop Consensus Panel 3. *Blood* 2011; **117**: 4701–5. doi: http://dx.doi.org/10.1182/blood-2010-10-299529
12. Durie BG, Salmon SE. A clinical staging system for multiple myeloma. Correlation of measured myeloma cell mass with presenting clinical features, response to treatment, and survival. *Cancer* 1975; **36**: 842–54. doi: http://dx.doi.org/10.1002/1097-0142(197509)36:3<842::AID-CNCR2820360303>3.0.CO;2-U
13. Durie BG. The role of anatomic and functional staging in myeloma: description of Durie/Salmon plus staging system. *Eur J Cancer* 2006; **42**: 1539–43. doi: http://dx.doi.org/10.1016/j.ejca.2005.11.037
14. Greipp PR, San Miguel J, Durie BG, Crowley JJ, Barlogie B, Bladé J, et al. International staging system for multiple myeloma. *J Clin Oncol* 2005; **23**: 3412–20. doi: http://dx.doi.org/10.1200/JCO.2005.04.242
15. Witt C, Borges AC, Klein K, Neumann HJ. Radiographic manifestations of multiple myeloma in the mandible: a retrospective study of 77 patients. *J Oral Maxillofac Surg* 1997; **55**: 450–453; discussion 454–5.
16. Grover SB, Dhar A. Imaging spectrum in sclerotic myelomas: an experience of three cases. *Eur Radiol* 2000; **10**: 1828–31. doi: http://dx.doi.org/10.1007/s003300000499
17. Edelstyn GA, Gillespie PJ, Grebbell FS. The radiological demonstration of osseous metastases. Experimental observations. *Clin Radiol* 1967; **18**: 158–62. doi: http://dx.doi.org/10.1016/S0009-9260(67)80010-2
18. Mahnken AH, Wildberger JE, Gehbauer G, Schmitz-Rode T, Blaum M, Fabry U, et al. Multidetector CT of the spine in multiple myeloma: comparison with MR imaging and radiography. *AJR Am J Roentgenol* 2002; **178**: 1429–36. doi: http://dx.doi.org/10.2214/ajr.178.6.1781429
19. Kusumoto S, Jinnai I, Itoh K, Kawai N, Sakata T, Matsuda A, et al. Magnetic resonance imaging patterns in patients with multiple myeloma. *Br J Haematol* 1997; **99**: 649–55. doi: http://dx.doi.org/10.1046/j.1365-2141.1997.4213236.x
20. Baur-Melnyk A, Buhmann S, Dürr HR, Reiser M. Role of MRI for the diagnosis and prognosis of multiple myeloma. *Eur J Radiol* 2005; **55**: 56–63. doi: http://dx.doi.org/10.1016/j.ejrad.2005.01.017
21. Tirumani SH, Shinagare AB, Jagannathan JP, Krajewski KM, Munshi NC, Ramaiya NH. MRI features of extramedullary myeloma. *AJR Am J Roentgenol* 2014; **202**: 803–10. doi: http://dx.doi.org/10.2214/AJR.13.10856
22. Moulopoulos LA, Dimopoulos MA, Alexanian R, Leeds NE, Libshitz HI. Multiple myeloma: MR patterns of response to treatment. *Radiology* 1994; **193**: 441–6. doi: http://dx.doi.org/10.1148/radiology.193.2.7972760
23. Weininger M, Lauterbach B, Knop S, Pabst T, Kenn W, Hahn D, et al. Whole-body MRI of multiple myeloma: comparison of different MRI sequences in assessment of different growth patterns. *Eur J Radiol* 2009; **69**: 339–45. doi: http://dx.doi.org/10.1016/j.ejrad.2007.10.025
24. Shortt CP, Gleeson TG, Breen KA, McHugh J, O'Connell MJ, O'Gorman PJ, et al. Whole-Body MRI *versus* PET in assessment of multiple myeloma disease activity. *AJR Am J Roentgenol* 2009; **192**: 980–6. doi: http://dx.doi.org/10.2214/AJR.08.1633
25. Song IC, Kim JN, Choi YS, Ryu H, Lee MW, Lee HJ, et al. Diagnostic and prognostic implications of spine magnetic resonance imaging at diagnosis in patients with multiple myeloma. *Cancer Res Treat* 2015; **47**: 465–72. doi: http://dx.doi.org/10.4143/crt.2014.010
26. Bartel TB, Haessler J, Brown TL, Shaughnessy JD Jr, van Rhee F, Anaissie E, et al. F18-fluorodeoxyglucose positron emission tomography in the context of other imaging techniques and prognostic factors in multiple myeloma. *Blood* 2009; **114**: 2068–76. doi: http://dx.doi.org/10.1182/blood-2009-03-213280
27. Mesguich C, Fardanesh R, Tanenbaum L, Chari A, Jagannath S, Kostakoglu L. State of the art imaging of multiple myeloma: comparative review of FDG PET/CT imaging in various clinical settings. *Eur J Radiol* 2014; **83**: 2203–23. doi: http://dx.doi.org/10.1016/j.ejrad.2014.09.012
28. Costelloe CM, Chuang HH, Madewell JE, Ueno NT. Cancer response criteria and bone metastases: RECIST 1.1, MDA and PERCIST. *J Cancer* 2010; **1**: 80–92. doi: http://dx.doi.org/10.7150/jca.1.80
29. Ghobrial IM, Gertz MA, Fonseca R. Waldenström macroglobulinaemia. *Lancet Oncol* 2003; **4**: 679–85. doi: http://dx.doi.org/10.1016/S1470-2045(03)01246-4
30. Moulopoulos LA, Dimopoulos MA, Varma DG, Manning JT, Johnston DA, Leeds NE, et al. Waldenström macroglobulinemia: MR imaging of the spine and CT of the abdomen and pelvis. *Radiology* 1993; **188**: 669–73. doi: http://dx.doi.org/10.1148/radiology.188.3.8351330
31. Banwait R, O'Regan K, Campigotto F, Harris B, Yarar D, Bagshaw M, et al. The role of 18F-FDG PET/CT imaging in Waldenström macroglobulinemia. *Am J Hematol* 2011; **86**: 567–72. doi: http://dx.doi.org/10.1002/ajh.22044
32. Wu H, Bui MM, Leston DG, Shao H, Sokol L, Sotomayor EM, et al. Clinical characteristics and prognostic factors of bone lymphomas: focus on the clinical significance of multifocal bone involvement by primary bone large B-cell lymphomas. *BMC cancer* 2014; **14**: 900. doi: http://dx.doi.org/10.1186/1471-2407-14-900
33. Limb D, Dreghorn C, Murphy JK, Mannion R. Primary lymphoma of bone. *Int Orthop* 1994; **18**: 180–3. doi: http://dx.doi.org/10.1007/BF00192476
34. Mulligan ME, McRae GA, Murphey MD. Imaging features of primary lymphoma of bone. *AJR Am J Roentgenol* 1999; **173**: 1691–7. doi: http://dx.doi.org/10.2214/ajr.173.6.10584821
35. Jawad MU, Schneiderbauer MM, Min ES, Cheung MC, Koniaris LG, Scully SP. Primary lymphoma of bone in adult patients. *Cancer* 2010; **116**: 871–9. doi: http://dx.doi.org/10.1002/cncr.24828
36. Krishnan A, Shirkhoda A, Tehranzadeh J, Armin AR, Irwin R, Les K. Primary bone lymphoma: radiographic-MR imaging correlation. *Radiographics* 2003; **23**: 1371–83; discussion 1384–77.
37. Mulligan ME, Kransdorf MJ. Sequestra in primary lymphoma of bone: prevalence and radiologic features. *AJR Am J Roentgenol* 1993; **160**: 1245–8. doi: http://dx.doi.org/10.2214/ajr.160.6.8498226
38. White LM, Schweitzer ME, Khalili K, Howarth DJ, Wunder JS, Bell RS. MR imaging of primary lymphoma of bone: variability of T2-weighted signal intensity. *AJR Am J Roentgenol* 1998; **170**: 1243–7. doi: http://dx.doi.org/10.2214/ajr.170.5.9574594

39. Stiglbauer R, Augustin I, Kramer J, Schurawitzki H, Imhof H, Radaszkiewicz T. MRI in the diagnosis of primary lymphoma of bone: correlation with histopathology. *J Comput Assist Tomogr* 1992; **16**: 248–53. doi: http://dx.doi.org/10.1097/00004728-199203000-00013
40. Conlan MG, Bast M, Armitage JO, Weisenburger DD. Bone marrow involvement by non-Hodgkin's lymphoma: the clinical significance of morphologic discordance between the lymph node and bone marrow. Nebraska Lymphoma Study Group. *J Clin Oncol* 1990; **8**: 1163–72.
41. Graham TS. The ivory vertebra sign. *Radiology* 2005; **235**: 614–15. doi: http://dx.doi.org/10.1148/radiol.2352021743
42. Klenk C, Gawande R, Uslu L, Khurana A, Qiu D, Quon A, et al. Ionising radiation-free whole-body MRI *versus* (18)F-fluorodeoxyglucose PET/CT scans for children and young adults with cancer: a prospective, non-randomised, single-centre study. *Lancet Oncol* 2014; **15**: 275–85. doi: http://dx.doi.org/10.1016/S1470-2045(14)70021-X
43. Stephane V, Samuel B, Vincent D, Joelle G, Remy P, Francois GG, et al. Comparison of PET-CT and magnetic resonance diffusion weighted imaging with body suppression (DWIBS) for initial staging of malignant lymphomas. *Eur J Radiol* 2013; **82**: 2011–17. doi: http://dx.doi.org/10.1016/j.ejrad.2013.05.042
44. Mayerhoefer ME, Karanikas G, Kletter K, Prosch H, Kiesewetter B, Skrabs C, et al. Evaluation of diffusion-weighted magnetic resonance imaging for follow-up and treatment response assessment of lymphoma: results of an 18F-FDG-PET/CT-controlled prospective study in 64 patients. *Clin Cancer Res* 2015; **21**: 2506–13. doi: http://dx.doi.org/10.1158/1078-0432.CCR-14-2454
45. Cortés-Romera M, Sabaté-Llobera A, Mercadal-Vilchez S, Climent-Esteller F, Serrano-Maestro A, Gámez-Cenzano C, et al. Bone marrow evaluation in initial staging of lymphoma: 18F-FDG PET/CT *versus* bone marrow biopsy. *Clin Nucl Med* 2014; **39**: e46–52. doi: http://dx.doi.org/10.1097/RLU.0b013e31828e9504
46. Chen-Liang TH, Martin-Santos T, Jerez A, Senent L, Orero MT, Remigia MJ, et al. The role of bone marrow biopsy and FDG-PET/CT in identifying bone marrow infiltration in the initial diagnosis of high grade non-Hodgkin B-cell lymphoma and Hodgkin lymphoma. Accuracy in a multicentre series of 372 patients. *Am J Hematol* 2015; **90**: 686–90. doi: http://dx.doi.org/10.1002/ajh.24044
47. Adams HJ, Kwee TC, de Keizer B, Fijnheer R, de Klerk JM, Littooij AS, et al. Systematic review and meta-analysis on the diagnostic performance of FDG-PET/CT in detecting bone marrow involvement in newly diagnosed Hodgkin lymphoma: is bone marrow biopsy still necessary? *Ann Oncol* 2014; **25**: 921–7. doi: http://dx.doi.org/10.1093/annonc/mdt533
48. Muzahir S, Mian M, Munir I, Nawaz MK, Faruqui ZS, Mufti KA, et al. Clinical utility of (1)(8)F FDG-PET/CT in the detection of bone marrow disease in Hodgkin's lymphoma. *Br J Radiol* 2012; **85**: e490–496. doi: http://dx.doi.org/10.1259/bjr/29583493
49. Berthet L, Cochet A, Kanoun S, Berriolo-Riedinger A, Humbert O, Toubeau M, et al. In newly diagnosed diffuse large B-cell lymphoma, determination of bone marrow involvement with 18F-FDG PET/CT provides better diagnostic performance and prognostic stratification than does biopsy. *J Nucl Med* 2013; **54**: 1244–50. doi: http://dx.doi.org/10.2967/jnumed.112.114710
50. Weiler-Sagie M, Kagna O, Dann EJ, Ben-Barak A, Israel O. Characterizing bone marrow involvement in Hodgkin's lymphoma by FDG-PET/CT. *Eur J Nucl Med Mol Imaging* 2014; **41**: 1133–40. doi: http://dx.doi.org/10.1007/s00259-014-2706-x
51. Sinigaglia R, Gigante C, Bisinella G, Varotto S, Zanesco L, Turra S. Musculoskeletal manifestations in pediatric acute leukemia. *J Pediatr Orthop* 2008; **28**: 20–8. doi: http://dx.doi.org/10.1097/BPO.0b13e31815ff350
52. Riccio I, Marcarelli M, Del Regno N, Fusco C, Di Martino M, Savarese R, et al. Musculoskeletal problems in pediatric acute leukemia. *J Pediatr Orthop B* 2013; **22**: 264–9. doi: http://dx.doi.org/10.1097/BPB.0b013e32835d731c
53. Pileri SA, Ascani S, Cox MC, Campidelli C, Bacci F, Piccioli M, et al. Myeloid sarcoma: clinico-pathologic, phenotypic and cytogenetic analysis of 92 adult patients. *Leukemia* 2007; **21**: 340–50. doi: http://dx.doi.org/10.1038/sj.leu.2404491
54. Shinagare AB, Krajewski KM, Hornick JL, Zukotynski K, Kurra V, Jagannathan JP, et al. MRI for evaluation of myeloid sarcoma in adults: a single-institution 10-year experience. *AJR Am J Roentgenol* 2012; **199**: 1193–8. doi: http://dx.doi.org/10.2214/AJR.12.9057
55. Lee EY, Anthony MP, Leung AY, Loong F, Khong PL. Utility of FDG PET/CT in the assessment of myeloid sarcoma. *AJR Am J Roentgenol* 2012; **198**: 1175–9. doi: http://dx.doi.org/10.2214/AJR.11.7743
56. Tefferi A. Myelofibrosis with myeloid metaplasia. *N Engl J Med* 2000; **342**: 1255–65. doi: http://dx.doi.org/10.1056/NEJM200004273421706
57. Mesa RA, Silverstein MN, Jacobsen SJ, Wollan PC, Tefferi A. Population-based incidence and survival figures in essential thrombocythemia and agnogenic myeloid metaplasia: an Olmsted County Study, 1976-1995. *Am J Hematol* 1999; **61**: 10–15. doi: http://dx.doi.org/10.1002/(SICI)1096-8652(199905)61:1<10::AID-AJH3>3.0.CO;2-I
58. Zhang B, Lewis SM. The splenomegaly of myeloproliferative and lymphoproliferative disorders: splenic cellularity and vascularity. *Eur J Haematol* 1989; **43**: 63–6. doi: http://dx.doi.org/10.1111/j.1600-0609.1989.tb01253.x
59. Kosmidis PA, Palacas CG, Axelrod AR. Diffuse purely osteolytic lesions in myelofibrosis. *Cancer* 1980; **46**: 2263–5. doi: http://dx.doi.org/10.1002/1097-0142(19801115)46:10<2263::AID-CNCR2820461025>3.0.CO;2-9
60. Mason BA, Kressel BR, Cashdollar MR, Bernath AM, Schechter GP. Periostitis associated with myelofibrosis. *Cancer* 1979; **43**: 1568–71. doi: http://dx.doi.org/10.1002/1097-0142(197904)43:4<1568::AID-CNCR2820430452>3.0.CO;2-B
61. Koch CA, Li CY, Mesa RA, Tefferi A. Nonhepatosplenic extramedullary hematopoiesis: associated diseases, pathology, clinical course, and treatment. *Mayo Clin Proc* 2003; **78**: 1223–33. doi: http://dx.doi.org/10.4065/78.10.1223
62. Guermazi A, de Kerviler E, Cazals-Hatem D, Zagdanski AM, Frija J. Imaging findings in patients with myelofibrosis. *Eur Radiol* 1999; **9**: 1366–75. doi: http://dx.doi.org/10.1007/s003300050850
63. Burrell SC, Fischman AJ. Myelofibrosis on F-18 FDG PET Imaging. *Clin Nucl Med* 2005; **30**: 674. doi: http://dx.doi.org/10.1097/01.rlu.0000178029.47624.66
64. Pour MC, Simon-Corat Y, Horne T. Diffuse increased uptake on bone scan: super scan. *Semin Nucl Med* 2004; **34**: 154–6. doi: http://dx.doi.org/10.1053/j.semnuclmed.2003.12.005